European Journal of Medicinal Chemistry 93 (2015) 121–134

Contents lists available at ScienceDirect

European Journal of Medicinal Chemistry

journal homepage: http://www.elsevier.com/locate/ejmech

Original article

When structure–affinity relationships meet structure–kinetics relationships: 3-((Inden-1-yl)amino)-1-isopropyl-cyclopentane-1-carboxamides as CCR2 antagonists

Maris Vilums [a], Annelien J.M. Zweemer [a], Farhana Barmare [b], Anouk M.F. van der Gracht [a], Dave C.T. Bleeker [a], Zhiyi Yu [a], Henk de Vries [a], Raymond Gross [b], Jeremy Clemens [b], Paul Krenitsky [b], Johannes Brussee [a], Dean Stamos [b], John Saunders [b], Laura H. Heitman [a], Adriaan P. IJzerman [a, *]

[a] Division of Medicinal Chemistry, Leiden Academic Centre for Drug Research, Leiden University, P.O. Box 9502, 2300 RA Leiden, The Netherlands
[b] Vertex Pharmaceuticals Incorporated, 11010 Torreyana Rd., San Diego, CA 92121, USA

ARTICLE INFO

Article history:
Received 28 August 2014
Received in revised form
29 January 2015
Accepted 31 January 2015
Available online 2 February 2015

Keywords:
CC chemokine receptor 2
CC chemokine receptor antagonists
Long residence time
Structure–kinetics relationships

ABSTRACT

Chemokine ligand 2 (CCL2) mediates chemotaxis of monocytes to inflammatory sites via interaction with its G protein–coupled receptor CCR2. Preclinical animal models suggest that the CCL2-CCR2 axis has a critical role in the development and maintenance of inflammatory disease states (e.g., multiple sclerosis, atherosclerosis, insulin resistance, restenosis, and neuropathic pain), which can be treated through inhibition of the CCR2 receptor. However, in clinical trials high–affinity inhibitors of CCR2 have often demonstrated a lack of efficacy. We have previously described a new approach for the design of high–affinity CCR2 antagonists, by taking their residence time (RT) on the receptor into account. Here, we report our findings on both structure–affinity relationship (SAR) and structure–kinetic relationship (SKR) studies for a series of 3-((inden-1-yl)amino)-1-isopropyl-cyclopentane-1-carboxamides as CCR2 antagonists. SAR studies showed that this class of compounds tolerates a vast diversity of substituents on the indenyl ring with only small changes in affinity. However, the SKR is affected greatly by minor modifications of the structure. The combination of SAR and SKR in the hit-to-lead process resulted in the discovery of a new high–affinity and long–residence–time CCR2 antagonist (compound **15a**, K_i = 2.4 nM; RT = 714 min).

1. Introduction

Chemokines are a class of endogenous pro-inflammatory proteins that act through activation and recruitment of leukocytes and other cell types in a range of inflammatory and non-inflammatory conditions. However, inappropriate overexpression

Abbreviations: Boc, tert-butyloxycarbonyl; CCL2, chemokine ligand 2; CCR2, chemokine receptor 2; CHAPS, 3-[(3-cholamidopropyl)dimethylammonio]-1-propanesulfonate; DBU, 1,8-diazabicycloundec-7-ene; DEA, diethylamine; DEAD, diethyl azodicarboxylate; DCM, dichloromethane; DiPEA, N,N-diisopropylethylamine; DMAP, N,N-dimethylaminopyridine; DMF, dimethylformamide; DPM, disintegrations per minute; EDTA, ethylenediaminetetraacetic acid; ESI, electrospray ionisation; FTMS, fourier transform mass spectrometer; G418, geneticin; HEPES, 4-(2-hydroxyethyl)piperazine-1-ethanesulfonic acid; hERG, human Ether-à-go-go-Related Gene; HPLC, high-performance liquid chromatography; HRMS, high resolution mass spectral analyses; INCB3344, N-[2-[[(3S,4S)-1-[4-(1,3-benzodioxol-5-yl)-4-hydroxycyclohexyl]-4-ethoxypyrrolidin-3-yl]amino]-2-oxoethyl]-3-(trifluoromethyl)benzamide; IPA, iso-propanol; KRI, kinetic rate index; LDA, lithium diisopropylamide; LC-MS, liquid chromatography – mass spectrometer; NEAA, non-essential amino acids; NMP, N-methylpyrrolidone; NMR, nuclear magnetic resonance; PEI, polyethylenimine; PEMB, 5-ethyl-2-methylpyridine borane; PyBrOP, bromo-tris-pyrrolidino phosphoniumhexafluorophosphate; RT, residence time; SAR, structure–affinity relationships; SFC, supercritical fluid chromatography; SKR, structure–kinetic relationships; TBDMS-Cl, tert-butyldimethylsilyl chloride; TFA, trifluoroacetic acid; THF, tetrahydrofuran; TLC, thin layer chromatography; TMS, tetramethylsilane; Tris, tris(hydroxymethyl)aminomethane; U2OS, human bone osteosarcoma cells; UPLC, ultra performance liquid chromatography; UV, ultraviolet.

* Corresponding author.
E-mail address: ijzerman@lacdr.leidenuniv.nl (A.P. IJzerman).

http://dx.doi.org/10.1016/j.ejmech.2015.01.063
0223-5234/

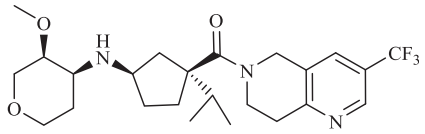

MK-0812
K_i = 0.55 nM
RT = 92 min

Fig. 1. Structure of MK-0812 [5].

of such proteins is implicated in a variety of disease conditions [1]. Both C–C Chemokine Ligand 2 (CCL2) and its cognate receptor C–C Chemokine Receptor 2 (CCR2) are involved in various autoimmune or inflammation-associated diseases. Blockade of the CCL2-CCR2 axis via either genetic or pharmacologic intervention has proven efficacious in animal models of multiple sclerosis, atherosclerosis, insulin resistance, restenosis, and neuropathic pain [2–4].

Fuelled by such promising preclinical data, there has been an increasing interest in advancing antagonists of CCR2 into clinical trials. Historically, small molecules tested have failed in clinical trials because of lack of efficacy, e.g., MK-0812 (orthosteric CCR2 antagonist for the treatment of rheumatoid arthritis and multiple sclerosis, Fig. 1) [5] and AZD-2423 (potent, orally bioavailable, non-competitive, negative allosteric modulator of the CCR2 chemokine receptor for treatment of neuropathic pain) [6]. A humanized anti-CCR2 antibody (MLN-1202) did not show efficacy either in patients with rheumatoid arthritis and multiple sclerosis [7]. However, administration of the antibody reduced the numbers of circulating monocytes in peripheral blood [8]. Moreover, a study of MLN-1202 in patients with risk factors for atherosclerosis demonstrated that treatment was able to reduce C–reactive protein levels [9]. This shows that CCR2 antagonism can have important biological effects in humans.

Perhaps, to be efficacious in treatment of CCR2–related diseases, high–affinity antagonism is not enough. Moreover, blockade of CCR2 can cause an increase in endogenous CCL2 levels [8] which could compete again with the administered drug. In recent years more and more attention has been devoted to an additional parameter in the drug discovery pipeline, i.e. drug–target residence time. It has been proposed that the lifetime of the ligand–receptor complex could be used as a possible indicator for drug efficacy and safety [10,11].

To probe this concept for CCR2 antagonists we determined the residence time of the failed clinical candidate MK-0812. In our assays it had a K_i value of 0.55 nM and a residence time of 92 min (see Fig. S4 and Table S1 in supporting materials). Previously we have generated high–affinity and longer–residence–time CCR2 antagonists based on a (1*S*,3*R*)-3-amino-N-(3,5-bis(trifluoromethyl)benzyl)-1-isopropylcyclopentane-1-carboxamide scaffold [12]. We explored different substituents and ring systems on the 3-amino group of the scaffold and observed that the longest residence time was found with an indane ring system. Although potent and long–residence–time compounds were identified in that study they were still very close to the residence time of MK-0812, thus we sought to prolong the RT and define more detailed structure–kinetics relationships for the CCR2 receptor. In the present study we evaluated different amide groups for the 3-((inden-1-yl)amino)-1-isopropyl-cyclopentane-1-carboxamide scaffold based on their RT and explored a broad chemical space around the indane ring system to define the SAR and SKR for 3-((inden-1-yl)amino)-1-isopropyl-cyclopentane-1-carboxamides as CCR2 antagonists.

2. Results and discussion

2.1. Chemistry

The synthesis of *N*-(3,5-bis(trifluoromethyl)benzyl)-3-((2,3-dihydro-1*H*-inden-1-yl)amino)-1-isopropylcyclopentane-1-carboxamide **1** and (1*S*,3*R*)-3-((tert-butoxycarbonyl)amino)-1-isopropylcyclopentane-1-carboxylic acid **2** was achieved following the approach reported earlier by our group [12]. From acid **2** and 1-(4-(trifluoromethyl)pyridin-2-yl)piperazine or 7-(trifluoromethyl)-1,2,3,4-tetrahydroisoquinoline hydrochloride via a peptide coupling reaction were generated amides **3** and **4** under bromo-tris-pyrrolidino phosphoniumhexafluorophosphate (PyBroP) conditions [13]. Subsequently, a solution of TFA in DCM (1:1) was used to remove the *N*-Boc protecting group which yielded amines **5** and **6**. Compounds **7**, **9**–**13** and **17a** – **22** were generated from amines **5** and **6** using an array of different indanones with the 5-ethyl-2-methylpyridine borane complex (PEMB) under conditions reported by Burkhardt and Coleridge (Scheme 1) [14]. In the

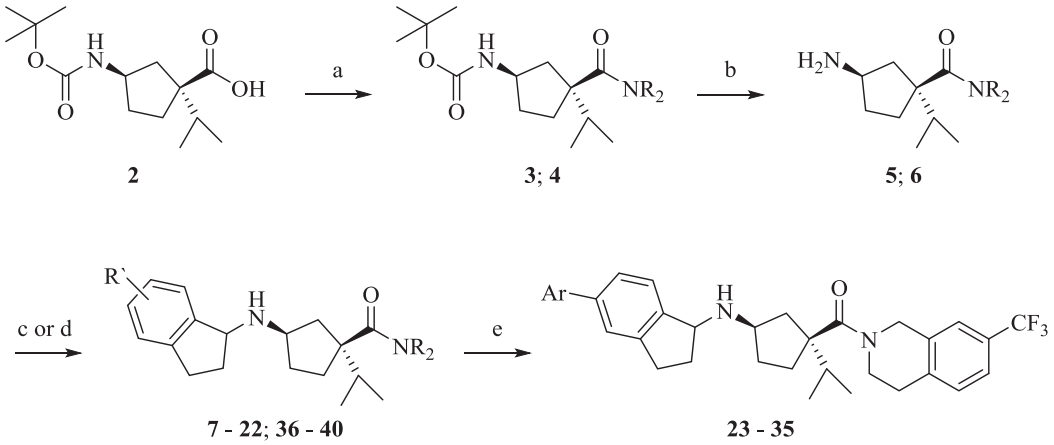

Scheme 1. Reagents and conditions: a) 1-(4-(trifluoromethyl)pyridin-2-yl)piperazine or 7-(trifluoromethyl)-1,2,3,4-tetrahydroisoquinoline hydrochloride, PyBrOP, DIPEA, DMAP, DCM, room temperature, 24 h, 82–90%; b) TFA, DCM, room temperature, 1 h, 90–98%; c) for array synthesis – corresponding indanone (1.05 equiv), 5-ethyl-2-methylpyridine borane (PEMB) (2.1 equiv), AcOH (1.05 equiv), NMP, 65 °C, 24 h, (compounds **7**; **9**–**13** and **17**–**22**); d) i) corresponding indanone (1,1 eq.), Ti(O-*i*-Pr)$_4$ (3 eq.), THF, 48 h, ii) $NaBH_4$, EtOH 16 h, room temperature, 8–41% (compounds **8**; **14**–**16** and **36**–**40**); e) array synthesis - compound **15**, corresponding aryl boronic acid, Na_2CO_3, $Pd(PPh_3)_4$, toluene/NMP/H_2O, 80 °C, 24 h, (compounds **23**–**35**).

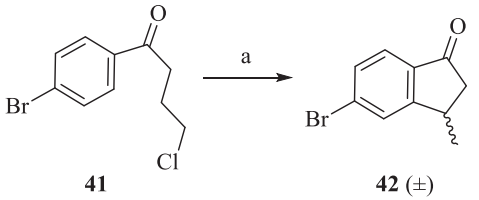

Scheme 2. Reagents and conditions: a) i) NaCl, $AlCl_3$, melt at 130 °C, ii) 4′-bromo-4-chloro-butyrophenone, 180 °C, 30 min, 91%.

case of the 5-CF_3 derivative (compound **17**) diastereomers were separated during the purification, however, only the first diastereomer to elute (**17a**) had a sufficient purity to be tested in bioassays. Compounds **8**, **14**–**16** and **36**–**40** were synthesized from **6** in a Ti(O*i*-Pr)$_4$ promoted reductive amination reaction with different indanones. Compounds **23**–**35** were synthesized via Suzuki–coupling of compound **15** with the corresponding arylboronic acids.

The synthesis of 3-Me; 5-Br indanone **42** was achieved by intramolecular cyclization of commercially available 1-(4-bromophenyl)-4-chlorobutan-1-one **41** following a procedure reported in the patent literature (Scheme 2) [15].

The 3-alkyl; 5-Br; 6-OMe indanones were synthesized as shown in Scheme 3. The reaction of 5-Br; 6-OMe indanone **43** with *tert*-butyldimethylchlorosilane and DBU in benzene gave ((6-bromo-5-methoxy-1*H*-inden-3-yl)oxy) (*tert*-butyl)dimethylsilane (**44**). Deprotonation of **44** with *n*-BuLi and reaction of the lithium salt with methyl iodide or ethyl iodide in THF and subsequent quenching of the reaction mixture with 12 M HCl resulted in 5-bromo-6-methoxy-3-alkyl-indanones (**45**, **46**).

The (1*S*)-5-bromo-3-methyl-2,3-dihydro-1*H*-indanol (**47**) and (1*R*)-5-bromo-3-methyl-2,3-dihydro-1*H*-indanol (**48**) were prepared via catalytic enantioselective reduction of racemic 5-bromo-3-methyl-2,3-dihydro-1*H*-indanone (**42**) using the (*R*)-methyl-CBS-oxazaborolidine and (*S*)-methyl-CBS-oxazaborolidine catalysts, respectively, with *N*,*N*-diethylaniline borane as reducing agent providing excellent enantioselectivity (Scheme 4) [16].

To prepare for the subsequent coupling, amine **6** was protected as the 2-nitrobenzenesulfonamide (**49**) (Scheme 5) [17]. The respective alcohols (**47**) and (**48**) when treated with (**49**) under Fukuyama–Mitsunobu conditions, resulted in N-alkylation to afford the 2-nitrobenzenesulfonamides (**50**) and (**51**) (Scheme 6). Selective deprotection of the 2-nitrobenzenesulfonamides (**50**) and (**51**) with thiophenol and K_2CO_3 gave the desired diastereomers **37a**, **37b**, **37c** and **37d** (Scheme 7).

2.2. Pharmacology

To determine their binding affinity all compounds were tested in a ^{125}I-CCL2 radioligand displacement assay on U2OS-CCR2 membrane preparations as described previously by our group [18]. Compounds with affinities better than or equal to 100 nM

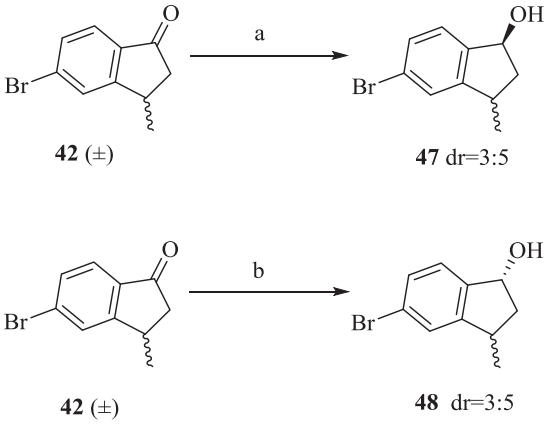

Scheme 4. Reagents and conditions: a) (*R*)-(+)-2-methyl-CBS-oxazaborolidine catalyst, *N*,*N*,diethylaniline borane, toluene, 3 h, room temperature, 97%; b) (*S*)-(+)-2-methyl-CBS-oxazaborolidine catalyst, *N*,*N*, diethylaniline borane, toluene, 3 h, room temperature, 99%.

were subsequently screened in a [^{3}H]INCB3344 dual point competition association assay on U2OS–CCR2 membrane preparations to determine their kinetic-rate-index (KRI), which served as an indicator for the magnitude of the RT. Compounds with a KRI > 1 were finally tested in the full competition association assay to determine the RT, as described previously by our group [12].

2.2.1. Structure–affinity relationships and structure–kinetics relationships

In the past few years several distinctly different amide groups have been disclosed for the general CCR2 scaffold of 3-amino-1-isopropylcyclopentanecarboxamides, with many final compounds displaying high and often very similar affinities (Fig. 2) [19–21]. In the current study we decided to keep the 3-((inden-1-yl)amino)-1-isopropyl-cyclopentane-1-carboxamide scaffold that was central in our previous report [12], and investigated the effect on affinity and RT of three different amide groups. When we changed the 3,5-bis(trifluoromethyl)benzyl group (compound **1**) (Table 1) to a 1-(4-(trifluoromethyl)pyridin-2-yl)piperazine group (compound **7**) the affinity was improved 3-fold ($p < 0.05$, Student's *t*-test), while a rigidification of the benzyl group into the 7-(trifluoromethyl)-1,2,3,4-tetrahydroisoquinoline group (compound **8**) yielded an even higher, 20-fold increase in affinity ($p < 0.005$, Student's *t*-test) (compounds **1**, **7** and **8**; $K_i = 50$ nM, 15 nM and 2.2 nM, respectively) (Fig. S2A in supporting materials). In kinetic tests of these compounds (kinetic rate index (KRI) [22] and RT) we learned that for longer receptor occupancy the smaller and less flexible tetrahydroisoquinoline was preferred (KRI = 0.8, 0.5 and 1.0; RT = 9.1, 8.3 and 21 min, for **1**, **7** and **8**, respectively) (Fig. S3A in supporting materials).

Encouraged by these results we decided to continue with compound **8** and investigate different substituents on the indenyl

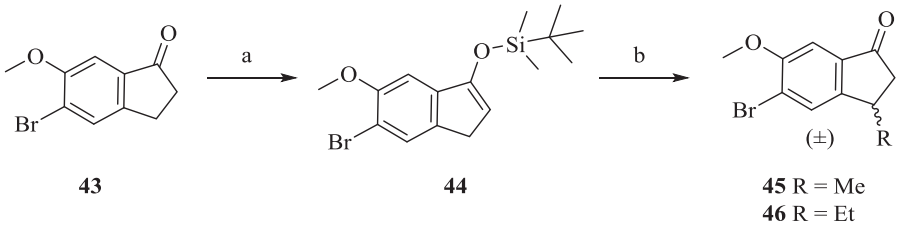

Scheme 3. Reagents and conditions: a) TBDMS-Cl, DBU, 0 °C → room temperature, 99%; b) i)LDA, 1 h, −78 °C → −35 °C, 1 h → −78 °C, corresponding alkyliodide, 2 h; ii) 12 M HCl, 82%.

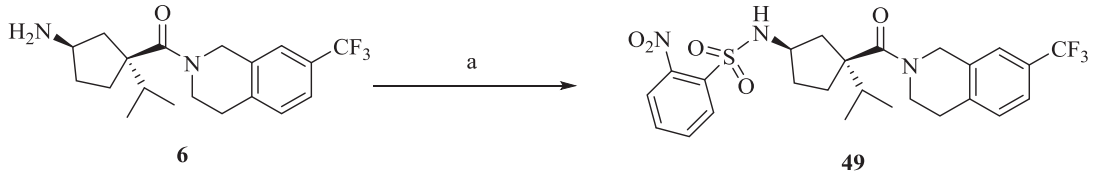

Scheme 5. Reagents and conditions: a) 2-nitrobenzenesulfonyl chloride, DIPEA, CH_2Cl_2, 1 h, room temperature, 98%.

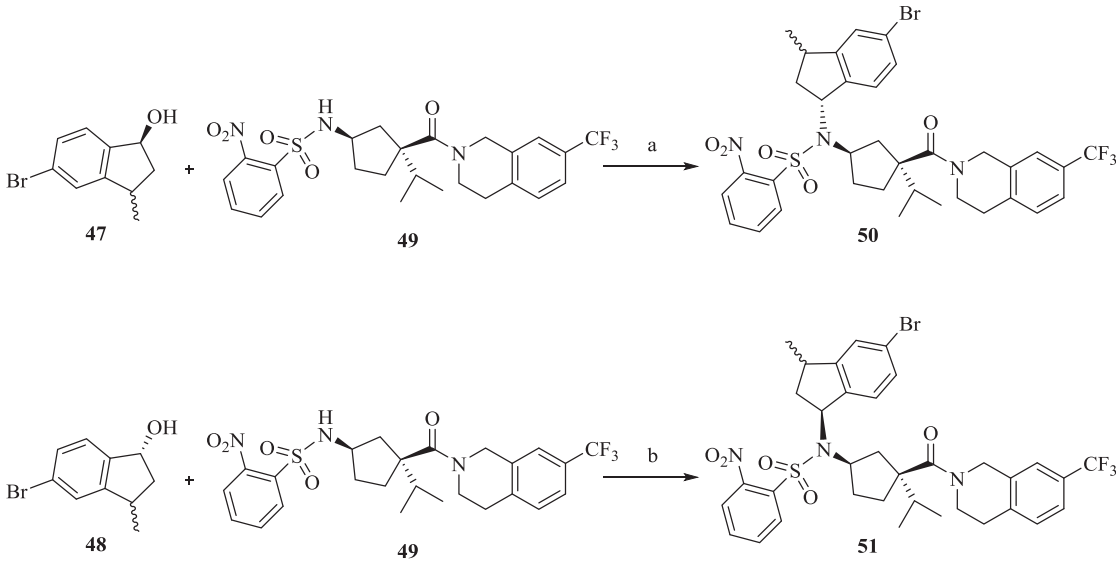

Scheme 6. Reagents and conditions: a) and b) DEAD, PPh3, THF, −78 °C to room temperature.

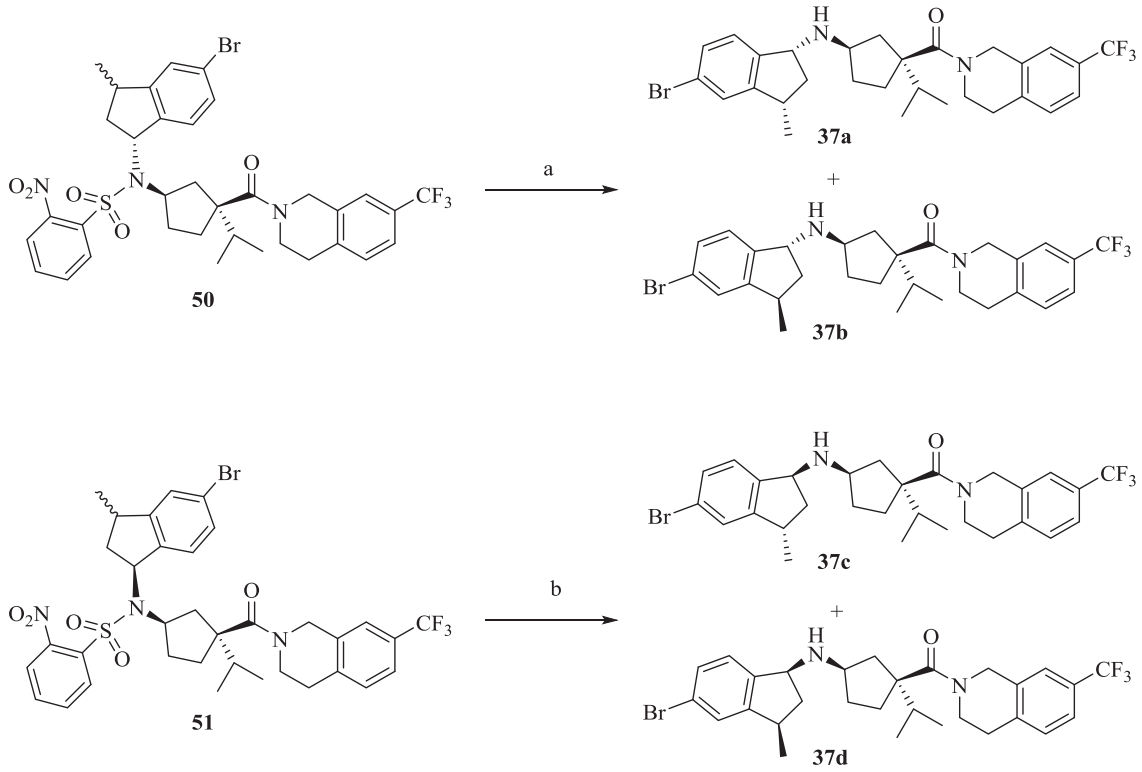

Scheme 7. Reagents and conditions: a) and b) PhSH, K_2CO_3, DMF, room temperature.

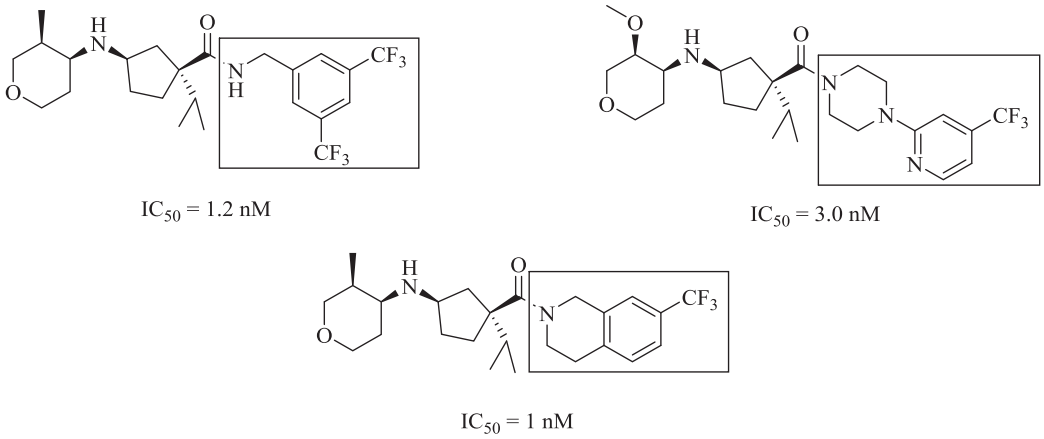

Fig. 2. CCR2 antagonists from Merck and Pfizer based on a 3-amino-1-isopropylcyclopentanecarboxamide scaffold with different amide groups [19–21].

group (Table 2). The rigidification of the right-hand side of the structure improved the affinity in general, while the order of substituents on the indenyl group was hardly affected when compared to our previous findings on the 3,5-bis(trifluoromethyl)benzylamide derivatives (compound **1**) [12]. Substitution on the 4-position decreased the affinity. Introduction of 4-Me (compound **9**) led to a 15-fold decrease ($p < 0.001$, Student's *t*-test). However, more polar groups were better tolerated. The 4-NH_2 substituent (compound **10**) maintained the affinity, while 4-CN and 4-OH groups were less tolerated (compounds **11** and **12**; $K_i = 15$ and 21 nM, respectively). Halogen substituents on the 5 position (compounds **13**, **14**, **15** and **16**) had little effect on affinity. Also an introduction of a CF_3 group (compound **17a**) - often considered as a bioisostere of chlorine – was tolerated. On the 6 position an electron donating methyl group (compound **18**) resulted in a decrease in affinity ($p < 0.05$, Student's *t*-test), while the electron withdrawing cyano (compound **19**) or the 6-Cl (compound **20**), both substituents were tolerated. However, the highest affinity compound **21** was obtained by double

Table 1
Binding Affinities, KRI and Residence Time of compounds **1**; **7** and **8**.

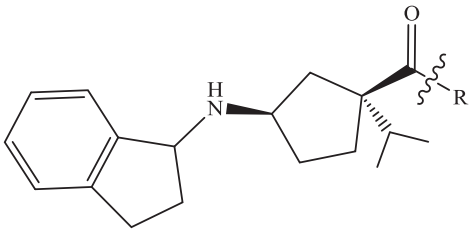

Compound number	R	K_i (nM) ± SEM ($n = 3$)	KRI ($n = 2$)	RT (min) ± SEM ($n = 3$)
1	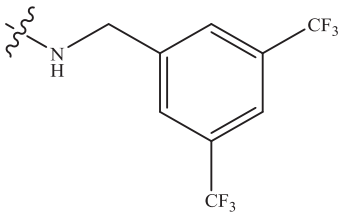	50 ± 8	0.8 (0.7/0.8)	9.1 ± 1.7
7	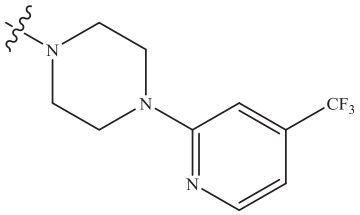	15 ± 1	0.5 (0.5/0.5)	8.3 ± 2.8
8	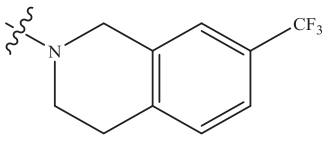	2.2 ± 0.6	1.0 (0.9/1.0)	21 ± 3

Table 2
Binding Affinities, KRI and Residence Time of compounds **8**–**22**.

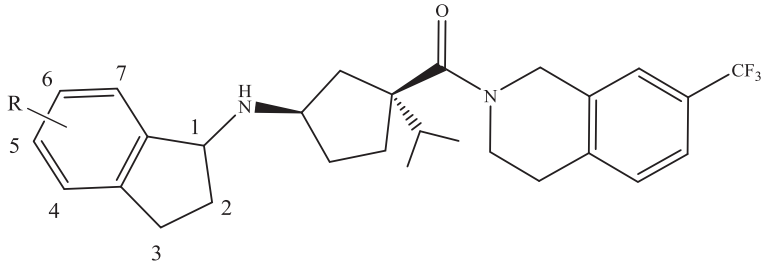

Compound number	R	K_i (nM) ± SEM ($n = 3$)	KRI ($n = 2$)	RT (min) ± SEM ($n = 3$)
8	H	2.2 ± 0.6	1.0 (0.9/1.0)	21 ± 3
9	4-Me	31 ± 2	0.7 (0.7/0.7)	–
10	4-NH_2	4.6 ± 1.0	0.7 (0.7/0.8)	–
11	4-CN	15 ± 5	0.6 (0.6/0.6)	–
12	4-OH	21 ± 3	0.7 (0.7/0.7)	–
13	5-F	4.9 ± 1.6	0.9 (0.9/0.9)	55 ± 6
14	5-Cl	1.6 ± 0.7	1.2 (1.0/1.3)	100 ± 20
15	5-Br	2.3 ± 0.6	1.3 (1.3/1.3)	213 ± 32
16	5-I	4.4 ± 0.9	1.3 (1.3/1.2)	103 ± 9
17a	5-CF_3	13 ± 5	1.4 (1.5/1.3)	667 ± 222
18	6-Me	23 ± 6	0.6 (0.6/0.5)	–
19	6-CN	13 ± 8	0.6 (0.6/0.7)	–
20	6-Cl	7.9 ± 2.0	0.6 (0.6/0.6)	–
21	5; 6-di-OMe	1.2 ± 0.3	1.0 (1.1/0.9)	63 ± 5
22	4,7-di OMe	49 ± 7	0.8 (0.8/0.8)	–

substitution on the 5 and 6 positions with methoxy groups. The corresponding regioisomer with 4,7-di-OMe (compound **22**) displayed a 40-fold decrease in affinity compared to compound **21** ($p < 0.005$, Student's *t*-test).

Testing these compounds in the high–throughput dual–point competition association assay showed that the abovementioned rigidification on the right–hand side of the molecule affects RT only for 5-substituted indenyl derivatives, with most of them having KRI values higher than unity. These compounds were tested in a full competition association assay and the highest affinity compound **21** had a RT of 63 min. Halogen substituents had size–dependent effects on KRI values. When tested for RT, indeed, increasing size correlated with longer residence times except for 5-I **16** where we observed a decrease in RT, as was the case for its affinity. However, compound **17a** (single diastereomer) displayed longer RT compared to its bioisostere the 5-Cl compound (**14**). All other compounds showed KRI values below unity and thus showed a behavior comparable to the benzyl derivatives reported earlier [12].

Next, we explored the 5 position by incorporating an additional aromatic system. Previously Xue et al. [23] had shown this approach to be successful in a pyrrolidine series of CCR2 antagonists. However, for our structures, an added unsubstituted phenyl ring (compound **23**) resulted in a dramatic decrease of affinity (Table 3). Adding a 2-Me group (compound **24**) yielded a small increase while 3-Me (compound **25**) did not improve the affinity compared to unsubstituted **23**. Incorporation of a cyano group on

Table 3
Binding Affinities, KRI and Residence Time of compounds **23**–**30**.

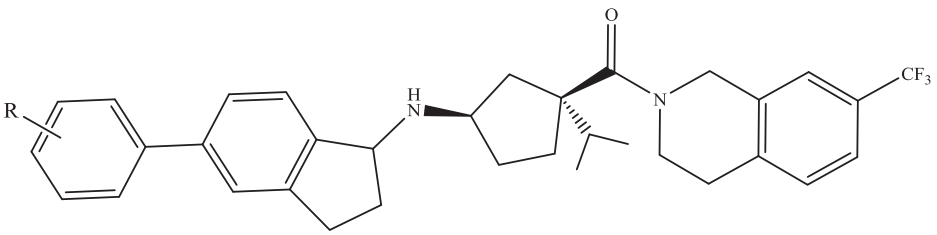

Compound number	R	K_i (nM) ± SEM ($n = 3$)	KRI ($n = 2$)
23	H	28%[a]	–
24	2-Me	46%[a]	–
25	3-Me	24%[a]	–
26	3-CN	55 ± 14	0.7 (0.7/0.7)
27	4-CN	11 ± 4.7	0.9 (0.8/1.0)
28	2-OMe	2%[a]	–
29	3-OMe	39 ± 6	0.8 (0.8/0.8)
30	4-OMe	75 ± 23	0.9 (0.9/0.9)

[a] Percent displacement at 1 μM ^{125}I-CCL2.

Table 4
Binding Affinities, KRI and Residence Time of compounds **31**–**35**.

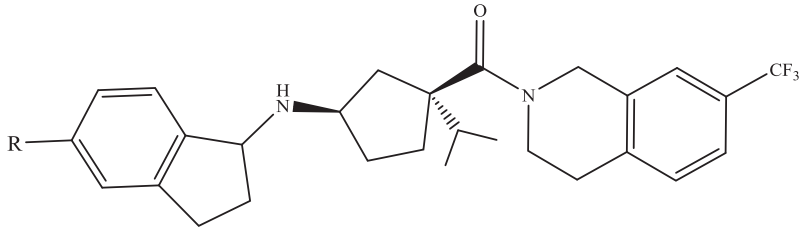

Compound number	R	K_i (nM) ± SEM ($n = 3$)	KRI ($n = 2$)
31	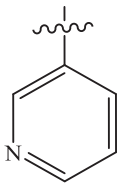	10 ± 5	0.7 (0.6/0.7)
32	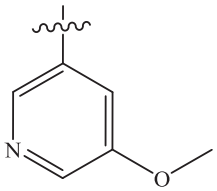	41 ± 8	0.8 (0.7/0.8)
33	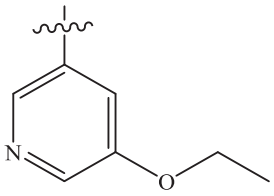	10 ± 4	0.5 (0.4/0.6)
34	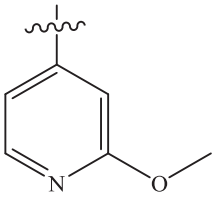	23 ± 7	0.6 (0.6/0.6)
35	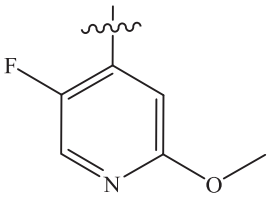	12 ± 1	0.8 (0.8/0.8)

the 3 or 4 position (compounds **26** and **27**) resulted in a regain of affinity into the nanomolar range. The same effect was observed with a methoxy group (compounds **29** and **30**). However, 2-OMe (compound **28**) was detrimental for affinity. These findings suggest that the space filling and hydrogen–accepting properties are more important for binding than the electronic properties of the substituents. Possible hydrogen bonding may also play a role when the phenyl ring was exchanged for 3-pyridine (compound **31**; $K_i = 10$ nM) (Table 4). Incorporation of a 2-OMe group (compound **32**) resulted in a decrease of affinity, with an affinity comparable to its phenyl analog **29**. Extending the substituent to an ethoxy group (compound **33**) is in accordance with the idea of space filling properties, as it yielded a gain in affinity compared to **32** ($p < 0.05$, Student's *t*-test). Changing the location of the nitrogen atom in the pyridine ring to the 4-position (compound **34**) was beneficial vs **32**. An additional gain in affinity was reached by incorporating a fluorine atom on the 5 position (compound **35**). In general, this series of compounds suggests there is enough space in the binding pocket to accommodate another aromatic ring with preferably hydrogen bond accepting properties. However, when these compounds were tested in the dual-point competition association assay none of them showed KRI values above 1.

Another approach to investigate SAR and SKR in more detail was based on the superimposition of structure **8** with the structure of MK-0483, which has been reported as a CCR2 antagonist with a receptor dissociation time ($T_{1/2}$) of over 9 h (Fig. 3) [24].

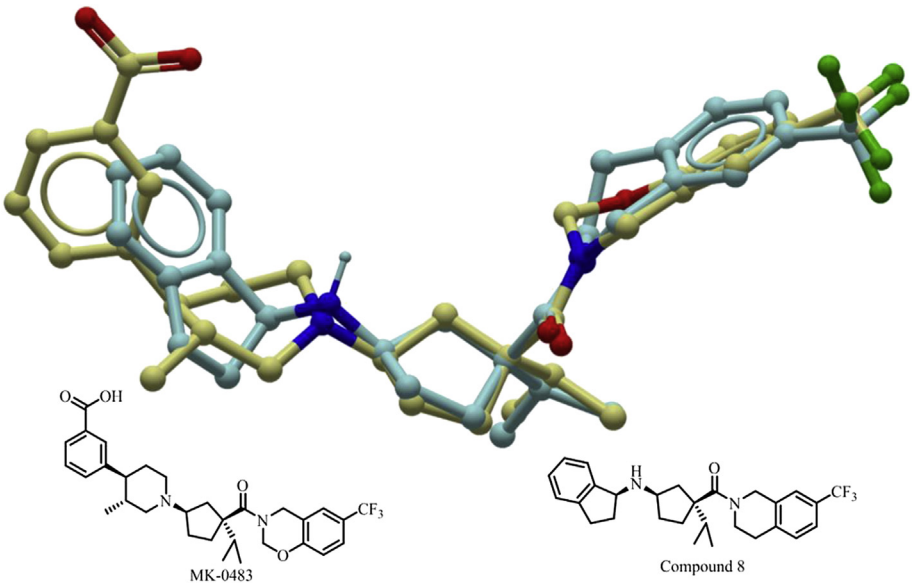

Fig. 3. Superimposition of MK-0483 (yellow) with compound **8** (cyan) using "ICM-Pro 3.7b, Molsoft LLC". (For interpretation of the references to color in this figure legend, the reader is referred to the web version of this article.)

In the superimposition, the 3-position of the indane ring of compound **8** overlaps with the 3 position of the piperidine ring of MK-0483. So we decided to incorporate a methyl group on the 3 position of the indenyl system to yield compound **36** (Table 5). This had a minor effect on the affinity, but caused a significant decrease in KRI value. However, the combination of a 3-Me and 5-Br substituent (compound **37**) yielded an increase in RT while affinity remained unchanged. This is an indication that the 3-Me group *per se* is not in direct contact with the receptor binding site. However, it could play an important role in shielding of a sub-pocket in combination with 5-Br; a similar idea was put forward by Schmidtke et al. [25] in calculations on hydrogen bond shielding. Intrigued by our findings, we decided to combine the substituents of the long RT compound **15** (5-Br) and highest affinity compound **21** (6-OMe) in one structure **38**. This combination yielded additional prolongation of the RT, while the affinity was not affected. Our next step was to make a hybrid of compounds **37** and **38** to incorporate 3-Me; 5-Br; 6-OMe substituents on the indenyl group in one compound **39** but it had no significant effect on the affinity. Next to this, we also extended the methyl group into an ethyl group (compound **40**). Unfortunately, these changes yielded 40-fold decreases in affinity ($p < 0.0001$, Student's *t*-test). However, the RT of the hybrid molecules were not affected when compared to 5-Br (compound **15**).

We then decided to separate compound **15** into diastereomers (Table 6) by preparative supercritical fluid chromatography (SFC). Similar to our previous findings [12] the first compound to elute also showed a higher affinity. However, the difference in affinity between the diastereomers was only 10-fold in the case of compounds **15a** and **15b** (Fig. S2A in supporting materials). In addition, compound **37** was resynthesized using a different method to yield all four diastereomers, which were separated (**37a-d**). *R*-diastereomers **37a** and **37b** retained high affinity, while *S*-diastereomers **37c** and **37d** had only sub-micromolar affinity values ($K_i = 1.7$, 4.6, 199 and 137 nM, respectively) (Fig. S2B in supporting materials).

In the RT measurements, a distinct difference was observed for

Table 5
Binding Affinities, KRI and Residence Time of compounds **36**–**40**.

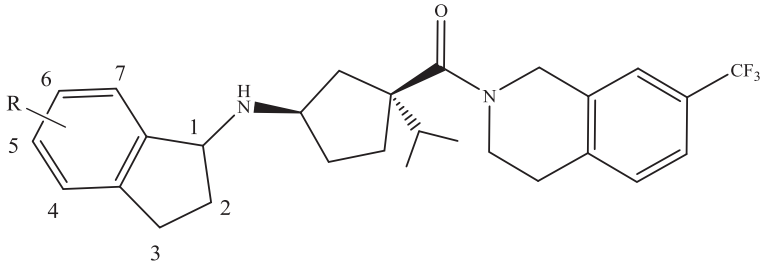

Compound number	R	K_i (nM) ± SEM ($n = 3$)	KRI ($n = 2$)	RT (min) ± SEM ($n = 3$)
36	3-Me	3.4 ± 0.5	0.7 (0.6/0.7)	–
37	5-Br, 3-Me	2.0 ± 0.2	1.3 (1.3/1.2)	345 ± 48
38	5-Br, 6-OMe	4.5 ± 1.0	1.3 (1.3/1.2)	323 ± 10
39	5-Br, 3-Me, 6-OMe	13 ± 4	1.5 (1.6/1.3)	238 ± 11
40	5-Br, 3-Et, 6-OMe	83 ± 5	1.3 (1.3/1.3)	179 ± 10

Table 6
Binding Affinities, KRI and Residence Time of separated diastereomers. (**15**, **15a**, **15b**, **37**, **37a**–**d**).

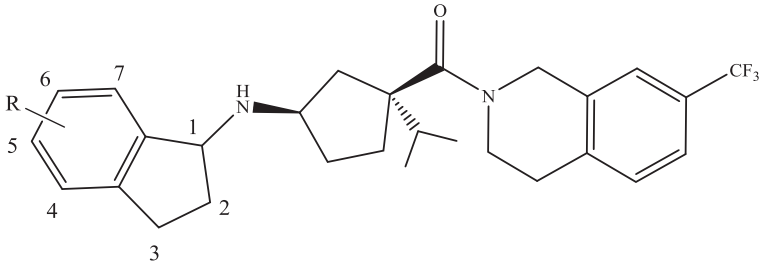

Compound number	R	K_i (nM) ± SEM ($n = 3$)	KRI ($n = 2$)	RT (min) ± SEM ($n = 3$)
15	5-Br	2.3 ± 0.6	1.3 (1.3/1.3)	213 ± 32
15a	5-Br	2.4 ± 1.2	1.7 (1.7/1.7)	714 ± 153
15b	5-Br	24 ± 9	0.8 (0.7/0.9)	15 ± 4
37	5-Br, 3-Me	2.0 ± 0.2	1.3 (1.3/1.2)	345 ± 48
37a	5-Br, 3-Me	1.7 ± 0.1	1.4 (1.4/1.4)	588 ± 208
37b	5-Br, 3-Me	4.6 ± 0.1	1.2 (1.2/1.1)	208 ± 35
37c	5-Br, 3-Me	199 ± 47	–	–
37d	5-Br, 3-Me	137 ± 15	–	–

the different diastereomers in the case of 7-(trifluoromethyl)-1,2,3,4-tetrahydroisoquinoline compounds on the amide part, quite the opposite of our previous findings for the flexible benzylamide derivatives [12]. The diastereomers of compound **15** had very different dissociation rate constants ($p < 0.05$, Student's *t*-test) while the association rate constants were similar (Table 7) (Fig. S3B in supporting materials). We succeeded in crystalizing compound **15a** for single–crystal X-ray diffraction analysis. Based on the crystallographic analysis, the absolute configuration of compound **15a** was the *R*-isomer (see Fig. S1 in supporting information). Apparently, the rigidification stabilizes specific interactions of the *R*-isomer in the binding site of the CCR2, which results in smaller dissociation rate constants. This is also in accordance with **37a** and **37b**, however, the additional methyl group on the indane ring should be positioned in the 3*R*-conformation (**37a**) resulting in a better affinity and longer RT than the 3*S*-diastereomer (**37b**) (Fig. S3C in supporting materials). The stereochemistry of **37a**–**d** was assigned using NOE experiments.

To confirm that our compounds are antagonists of CCR2 we performed a G protein-dependent functional assay. We used a [^{35}S] GTPγS binding assay on U2OS-CCR2 membranes, where we measured G protein activation by CCL2 in the absence and presence of 10 μM of a selection of antagonists (Fig. 4). Compounds **15a**, **15b**, **17a**, **37a** and **37b** all inhibited CCL2-induced G protein activation, hence they are antagonists of CCR2.

3. Conclusion

We have evaluated the SAR and SKR of 3-((inden-1-yl)amino)-1-isopropyl-cyclopentane-1-carboxamide derivatives as CCR2 antagonists. On the right-hand side of the molecule the 7-(trifluoromethyl)-1,2,3,4-tetrahydroisoquinoline group is optimal to increase residence time. On the left-hand side, the indane ring can accommodate very different substituents, as many compounds maintain nanomolar affinity. However, lipophilic and electron-withdrawing substituents (e.g. Cl, Br, I, CF_3) on the 5-position of the indane ring are crucial for long residence time. Moreover a comparison between e.g., compounds **8** and **15a** demonstrates that affinity and residence time do not necessarily correlate and it stresses the importance of additional screening for residence time in the early stages of drug discovery. In addition, small changes of the structure can have a big impact on residence time, e.g., the incorporation of a 5-Br (**15a**) substituent yielded a more than 30-fold increase in residence time (714 min). From this perspective compound **15a** should be evaluated in CCR2–related disease animal models to assess the usefulness of prolonged inhibition of CCR2. In general, this work provides methodology to retrieve the kinetic parameters from the vast number of high affinity compounds in the early stages of the drug discovery process, which could help to provide better drug candidates for the later stages of drug development.

4. Experimental section

4.1. Chemistry

All solvents and reagents were purchased from commercial sources and were of analytical grade. Demineralized water is simply referred to as H_2O, because it was used in all cases, unless stated otherwise (i.e., brine). ^{1}H and ^{13}C NMR spectra were recorded on a

Table 7
Kinetic data of **15a**, **b**, **17a** and **37a**, **b** compounds.

Compound number	K_i (nM) ± SEM (n = 3)	k_{on} (nM^{-1} min^{-1}) ± SEM ($n = 3$)	k_{off} (min^{-1}) ± SEM ($n = 3$)	RT (min) ± SEM ($n = 3$)
15a	2.4 ± 1.2	0.0080 ± 0.0011	0.0014 ± 0.0003	714 ± 153
15b	24 ± 9	0.0059 ± 0.001	0.066 ± 0.017	15 ± 4
17a	13 ± 5	0.0032 ± 0.0004	0.0015 ± 0.0005	667 ± 222
37a	1.7 ± 0.1	0.0044 ± 0.0003	0.0017 ± 0.0006	588 ± 208
37b	4.6 ± 0.1	0.0026 ± 0.0006	0.0048 ± 0.0008	208 ± 35

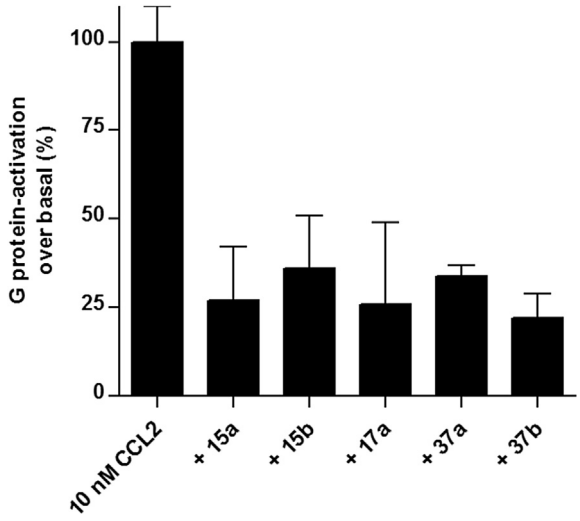

Fig. 4. G protein-activation by 10 nM CCL2 measured in a [^{35}S]GTPγS binding assay on U2OS-CCR2 membranes in the absence and presence of 10 μM of a selection of compounds.

Bruker AV 400 liquid spectrometer (^{1}H NMR, 400 MHz; ^{13}C NMR, 100 MHz) or on a Bruker 500 MHz Avance III NMR spectrometer (compounds **15a**, **b** and **37a** − **d**) at ambient temperature. Chemical shifts are reported in parts per million (ppm), are designated by δ, and are downfield to the internal standard tetramethylsilane (TMS). Coupling constants are reported in hertz and are designated as *J*. Analytical purity of the final compounds was determined by high-performance liquid chromatography (HPLC) with a Phenomenex Gemini 3 μm C18 110A column (50 × 4.6 mm, 3 μm), measuring UV absorbance at 254 nm. The sample preparation and HPLC method for compounds **8**; **14**–**16** and **36**–**40** were as follows: 0.3–0.8 mg of compound was dissolved in 1 mL of a 1:1:1 mixture of CH_3CN/H_2O/*t*-BuOH and eluted from the column within 15 min at a flow rate of 1.3 mL/min. The elution method was set up as follows: 1–4 min isocratic system of H_2O/CH_3CN/1% TFA in H_2O, 80:10:10, from the 4th min, a gradient was applied from 80:10:10 to 0:90:10 within 9 min, followed by 1 min of equilibration at 0:90:10 and 1 min at 80:10:10. All compounds showed a single peak at the designated retention time and are at least 95% pure. Enantiomeric excess was accomplished using chiral SFC. For **47** and **48** the column was Chiralpak AD-H (250 × 4.6 mm), 5 μm. The mobile phase condition of 10% MeOH with 20 mM NH_3 and 90% CO_2 was applied at a flow rate of 3.0 mL/min at 254 nm. For **37a** and **37b** the column was Phenomenex Lux-4 (250 × 4.6 mm), 5 μm. The mobile phase condition of 20% *i*-propanol (IPA) with 1.0% DEA and 80% CO_2 was applied at a flow rate of 3.0 mL/min at 254 nm. For **37c** and **37d** the column was Regis RR-Whelko (250 × 4.6 mm), 5 μm. The mobile phase condition of 25% IPA with 1.0% diethylamine (DEA) and 75% CO_2 was applied at a flow rate of 3.0 mL/min at 254 nm. High-resolution mass spectral analyses (HRMS) were performed on LTQ-Orbitrap FTMS operated in a positive ionization mode with an electrospray ionization (ESI) source, with the following conditions: mobile phase A, 0.1% formic acid in water; mobile phase B, 0.08% formic acid in CH_3CN; gradient, 10–80% B in 26 min; and flow rate, 0.4 mL/min. Preparative HPLC (for compounds **7**; **9**–**13** and **18**–**35**) was performed on a Waters Auto Purification HPLC–ultraviolet (UV) system with a diode array detector using a Luna C18 Phenomenex column (75 × 30 mm, 5 μm), and a linear gradient from 1 to 99% of mobile phase B was applied. Mobile phase A consisted of 5 mM HCl solution, and mobile phase B consisted of acetonitrile. The flow rate was 50 mL/min. Liquid chromatography–mass spectrometry (LC–MS) analyses were performed using an Onyx C18 monolithic column (50 × 4.6 mm, 5 μm), and a linear gradient from 1 to 99% mobile phase B was applied. Mobile phase A consisted of 0.05% TFA in water, and mobile phase B consisted of 0.035% TFA in acetonitrile. The flow rate was 1.2 mL/min. Separations of enantiomers were accomplished using chiral SFC. The column was Phenomenex Lux-4 (250 × 10 mm, 5 μm). The mobile phase condition of 10% MeOH with 20 mM NH_3 and 90% CO_2 was applied at a flow rate of 10 mL/min. Optical rotations were measured in ethanol at 20 °C on a Perkin–Elmer polarimeter (Wavelength = 589 nm). The single crystal X-ray diffraction studies were carried out on a Bruker Kappa APEX-II CCD diffractometer equipped with Mo K_α radiation (λ = 0.71073 Å). Thin-layer chromatography (TLC) was routinely consulted to monitor the progress of reactions, using aluminum-coated Merck silica gel F^{254} plates. Purification by column chromatography was achieved by use of Grace Davison Davisil silica column material (LC60A, 30–200 μm). The procedure for a series of similar compounds is given as a general procedure for all within that series, annotated by the numbers of the compounds.

Synthesis of (1*S*,3*R*)-3-(tert-butoxycarbonylamino)-1-isopropylcyclopentanecarboxylic acid (**2**) was achieved following the synthetic approach reported earlier by our group [12].

*4.1.1. General procedure for the synthesis of compounds **3** and **4***

Compound **2** (1 equiv) was dissolved in 25 mL DCM. To this mixture the corresponding amine (1 equiv) was added and subsequently DiPEA (3 equiv), PyBrOP (1 equiv) and DMAP (0.8 equiv). The reaction mixture was stirred for 24 h at room temperature. The product was partitioned between DCM and 1 M citric acid solution in water and then with DCM/1 M NaOH. The organic layer was dried with $MgSO_4$ and evaporated. The product was purified by column chromatography (0–100% ethyl acetate in DCM).

*4.1.1.1. tert-Butyl ((1R,3S)-3-isopropyl-3-(4-(4-(trifluoromethyl)pyridin-2-yl)piperazine-1-carbonyl)cyclopentyl)carbamate (**3**) [20].* Yield = 90%. ^{1}H NMR (400 MHz, $CDCl_3$) δ: 8.22 (d, *J* = 4.8 Hz, 1H), 6.77–6.72 (m, 2H), 4.94 (br s, 1H), 3.82 (br s, 1H), 3.70–3.61 (m, 4H), 3.59–3.45 (m, 4H), 2.11–1.90 (m, 3H), 1.80–1.61 (m, 4H), 1.31 (s, 9H), 0.81–0.72 (m, 6H) ppm.

*4.1.1.2. tert-Butyl ((1R,3S)-3-isopropyl-3-(7-(trifluoromethyl)-1,2,3,4-tetrahydroisoquinoline-2-carbonyl)cyclopentyl)carbamate (**4**) [26].* Yield = 82%. ^{1}H NMR (400 MHz, $CDCl_3$) δ: 7.45 (d, *J* = 7.6 Hz, 1H), 7.40 (s, 1H), 7.28 (d, *J* = 7.6, 1H), 4.97–4.61 (m, 3H), 4.00–3.73 (m, 3H), 2.94 (br s, 2H), 2.30–2.05 (m, 3H), 1.88–1.67 (m, 3H), 1.59 (br s, 1H), 1.42 (s, 9H), 0.91–0.84 (m, 6H) ppm.

*4.1.2. ((1S,3R)-3-Amino-1-isopropylcyclopentyl) (4-(4-(trifluoromethyl)pyridin-2-yl)piperazin-1-yl)methanone (**5**) [20]*

Trifluoroacetic acid (4 mL) was added to a solution of compound **3** (1.20 g, 2.48 mmol) in 10 mL of DCM. The reaction mixture was stirred for 2 h at room temperature. The reaction mixture was neutralized with 1 M NaOH and extracted with DCM. The organic layer was dried with $MgSO_4$, filtered, and evaporated to give the product as yellow crystals (0.86 g, 90%). ^{1}H NMR (400 MHz, $CDCl_3$) δ: 8.20 (d, *J* = 4.8 Hz, 1H), 6.77–6.72 (m, 2H), 3.72–3.38 (m, 8H), 3.20–3.10 (m, 1H), 2.45–2.30 (m, 1H), 2.07–1.90 (m, 2H), 1.80–1.35 (m, 4H), 0.83–0.70 (m, 6H) ppm.

*4.1.3. ((1S,3R)-3-Amino-1-isopropylcyclopentyl) (7-(trifluoromethyl)-3,4-dihydroisoquinolin-2(1H)-yl)methanone (**6**) [26]*

Trifluoroacetic acid (10 mL) was added to a solution of compound **4** (3.27 g, 7.2 mmol) in 10 mL of DCM. The reaction mixture was stirred for 1 h at room temperature. The reaction mixture was

neutralized with 1 M NaOH and extracted with DCM. The organic layer was dried with $MgSO_4$, filtered, and evaporated to give the product as yellow crystals (2.50 g, 98%). ^{1}H NMR (400 MHz, $CDCl_3$) δ: 7.40 (d, J = 7.6 Hz, 1H), 7.36 (s, 1H), 7.24 (d, J = 7.6, 1H), 4.76 (s, 2H), 3.81 (br s, 2H), 3.32–3.22 (m, 1H), 2.91 (br s, 2H), 2.53–2.45 (m, 1H), 2.18–1.73 (m, 4H), 1.69–1.60 (m, 1H), 1.40–1.35 (m, 1H), 0.91–0.84 (m, 6H) ppm.

4.1.4. General procedure for the synthesis of compounds **7**, **9**–**13** and **18**–**23**

To a series of 1.5 mL glass tubes was added amine **5** or **6** in NMP (0.95 M, 0.095 mmol), followed by solutions of different indanones (0.5 M, 0.1 mmol) in NMP, and these mixtures were subsequently treated with acetic acid (0.1 mmol), followed by 5-ethyl-2-methyl-pyridine borane (PEMB) (0.2 mmol). The reaction mixture was heated at 65 °C on a reaction block for 24 h. The reaction mixtures were purified directly using an automated mass-guided reverse-phase HPLC, and product containing fractions were concentrated to give final products of >90% purity as judged by LC–MS (average of 220 and 254 nm traces).

4.1.5. General procedure for the synthesis of compounds **8**, **14**–**16** and **36**–**40**

In a 5 mL glass tube, amine **6** (1 equiv) dissolved in 1 mL of dry THF, and the corresponding indanone (1.2 equiv) dissolved in 1 mL of dry THF were loaded. Mixture was flushed with nitrogen gas and the tube was capped. Through the septa Ti(O-*i*-Pr)$_4$ (3 equiv) was added and the reaction mixture was stirred for 48 h at room temperature. Then the tube was decapped and $NaBH_4$ (5 equiv) and 0.5 mL of absolute EtOH were added, and stirred for 16 h. The reaction mixture was quenched with H_2O and resulting inorganic precipitate was filtered off and washed with DCM. The filtrate was extracted with DCM/H_2O. The organic layer was dried with $MgSO_4$ and evaporated. The product was purified by column chromatography (40% ethyl acetate in DCM).

4.1.5.1. ((1S,3R)-3-((2,3-dihydro-1H-inden-1-yl)amino)-1-isopropylcyclopentyl) (7-(trifluoromethyl)-3,4-dihydroisoquinolin-2(1H)-yl)methanone (**8**).

Yield = 34%. ^{1}H NMR (400 MHz, $CDCl_3$) δ: 7.57–7.37 (m, 2H), 7.37–7.10 (m, 5H), 4.91–4.75 (m, 2H), 4.37–4.20 (m, 1H), 3.85 (s, 2H), 3.36–3.20 (m, 1H), 3.09–2.88 (m, 3H), 2.88–2.74 (m, 1H), 2.58 (br s, 1H), 2.49–2.33 (m, 1H), 2.25–1.87 (m, 4H), 1.87–1.72 (m, 2H), 1.72–1.56 (m, 1H), 1.48–1.35 (m, 1H), 1.01–0.79 (m, 6H) ppm. LC–MS: 471$^+$; t_R: 9.79 min.

4.1.6. ((1S,3R)-1-isopropyl-3-((5-(trifluoromethyl)-2,3-dihydro-1H-inden-1-yl)amino)cyclopentyl) (7-(trifluoromethyl)-3,4-dihydroisoquinolin-2(1H)-yl)methanone (**17a**)

In a 50 mL round–bottom flask, to a solution of 1 equivalent of amine **6** in anhydrous methanol was added 1 equivalent of 5-(trifluoromethyl)-2,3-dihydro-1*H*-inden-1-one which was subsequently treated with 2 equivalents of acetic acid, followed by 4 equivalents of 5-ethyl-2-methyl-pyridine borane (PEMB). The reaction mixture was heated at 65 °C for 24 h. Reaction mixture was monitored by reverse phase UPLC (t_R: 0.53) and was carefully quenched with concentrated HCl, then water was added to the reaction mixture and extracted with dichloromethane. The combined organic layer was washed with brine, dried over Na_2SO_4, and concentrated *in vacuo*. Reraction mixture was purified by flash chromatography (0–20 % CH_2Cl_2/MeOH) to afford product **17** (mixture of diastereomers). Further purification by reverse-phase HPLC using a gradient from 1 to 99% mobile phase B (mobile phase A = 0.1% HCl in water, mobile phase B = 0.1% HCl in CH_3CN) resulted in the separation of the two diastereomers **17 a** and **17 b** as HCl salt. Yield: **17a** = 19.5%, 96% purity,UPLC-MS: 539$^+$; t_R: 1.45 min and **17b** = 8.0%, 83% purity, UPLC-MS: 539$^+$; t_R: 1.48 min **17a**: ^{1}H NMR (400 MHz, $CDCl_3$) δ: 10.09 (s, 1H), 9.24 (s, 1H), 7.85 (d, J = 8.0 Hz, 1H), 7.57 (s, 1H), 7.50 (d, J = 7.7 Hz, 1H), 7.46–7.38 (m, 1H), 7.35 (s, 1H), 7.29–7.20 (m, 1H), 4.90–4.62 (m, 3H), 3.84 (s, 1H), 3.68 (t, J = 8.7 Hz, 1H), 3.48 (q, J = 7.8, 7.0 Hz, 1H), 2.93 (ddt, J = 19.3, 11.4, 5.0 Hz, 3H), 2.68 (d, J = 14.1 Hz, 1H), 2.64–2.37 (m, 3H), 2.18–1.97 (m, 3H), 1.92 (dd, J = 14.2, 7.4 Hz, 1H), 1.80 (s, 1H), 1.68 (d, J = 12.1 Hz, 1H), 0.84 (dd, J = 20.0, 6.6 Hz, 6H) ppm.

4.1.7. General procedure for the synthesis of compounds **23**–**35**

To a series of 1.5 mL glass tubes was added **15** in toluene (0.1 mmol) followed by solutions of different aryl boronic acids (0.5 M, 0.2 mmol) in NMP and these mixtures were subsequently treated with Na_2CO_3 solution (1 M, 0.2 mmol) followed by $Pd(PPh_3)_4$ in toluene (0.05 eq, 0.005 mmol). The reaction mixtures (0.15 M) were capped and heated at 80 °C on a reaction block overnight. The reaction mixtures were purified directly using an automated mass–guided reverse phase–HPLC, and product containing fractions were concentrated to give final products >90% purity as judged by LC-MS (average of 220 nm and 254 nm traces).

4.1.8. 5-bromo-3-methyl-2,3-dihydro-1H-inden-1-one (**42**)

[15] In a 50 mL round-bottom flask NaCl (3.7 g, 63.0 mmol) and $AlCl_3$ (15.0 g, 115 mmol) were loaded and heated at 130 °C until completely melted. Next, 4′-bromo-4-chloro-butyrophenone (**41**) (3.0 g, 11.5 mmol) was added and the reaction mixture was heated at 180 °C for 30 min. After cooling to room temperature, the reaction mixture was slowly poured on an ice/1 N HCl mixture – an exothermic reaction was observed. The reaction mixture was extracted with DCM, dried with $MgSO_4$ and the organic solvent was evaporated to yield 2.35 g (yield 91%, with 90% purity) of light brown crystals which were used in the next step without purification. ^{1}H NMR (400 MHz, $CDCl_3$) δ: 7.70 (s, 1H), 7.61 (d, J = 8.4 Hz, 1H), 7.54 (d, J = 8.4 Hz, 1H), 3.50–3.40 (m, 1H), 2.96 (ABX, J = 19.2 Hz^a, J = 7.6 Hz^b, 1H), 2.30 (ABX, J = 18.8 Hz^a, J = 3.6 Hz^b, 1H), 1.43 (d, J = 7.2 Hz, 3H) ppm.

4.1.9. ((6-Bromo-5-methoxy-1H-inden-3-yl)oxy) (tert-butyl) dimethylsilane (**44**)

In a 25 mL round–bottom flask 5-bromo-6-methoxy-2,3-dihydro-1*H*-inden-1-one (**43**) (0.96 g, 4.0 mmol) was dissolved in 8 mL of toluene and cooled to 0 °C. TBDMS-Cl solution in toluene (1.95 mL, 6.5 mmol) was added, followed by dropwise addition of DBU (1.12 mL, 7.5 mmol). The reaction mixture was stirred at 0 °C for 10 min and continued to be stirred at room temperature for 7 days. The reaction mixture was extracted with Et_2O/H_2O, dried with $MgSO_4$, and evaporated. Yield = 1.40 g (98%), which was used in the next step without purification. ^{1}H NMR (400 MHz, $CDCl_3$) δ: 7.55 (s, 1H), 6.94 (s, 1H), 5.47 (t, J = 2.4 Hz, 1H), 3.96 (s, 3H), 3.22 (d, J = 2.4 Hz, 2H), 1.05 (s, 9H), 0.29 (s, 6H) ppm.

4.1.10. 5-bromo-6-methoxy-3-methyl-2,3-dihydro-1H-inden-1-one (**45**)

In a 20 mL reaction tube a 2 M solution of LDA (0.6 mL, 1.2 mmol) in THF/heptane/ethylbenzene was mixed with 5 mL of dry THF. The reaction mixture was cooled down to −78 °C and compound **44** (0.35 g, 1 mmol) (dissolved in 1 mL of dry THF) was added. The reaction mixture was warmed to −35 °C during 1 h and then cooled back to −78 °C. Methyl iodide (0.08 mL, 1.3 mmol) was added and the reaction mixture was warmed to room temperature over 2 h and left stirring overnight. 37% HCl in water (0.27 mL, 3.2 mmol) was added and this mixture was stirred for 3 h. The reaction mixture was extracted with DCM/H_2O, dried with $MgSO_4$, and evaporated. The product was purified by column chromatography with DCM as eluent. Yield = 0.21 g (82%). ^{1}H NMR (400 MHz, $CDCl_3$)

δ: 7.61 (s,1H), 7.03 (s, 1H), 3.83 (s, 3H), 3.35–3.25 (m, 1H), 2.85 (ABX, $J = 18.8$ Hz^a, $J = 7.6$ Hz^b, 1H), 2.18 (ABX, $J = 19.2$ Hz^a, $J = 3.2$ Hz^b, 1H), 1.29 (d, $J = 7.2$ Hz, 3H) ppm.

4.1.11. 5-bromo-6-methoxy-3-ethyl-2,3-dihydro-1H-inden-1-one (**46**)

In a 20 mL reaction tube a 2 M solution of LDA (0.6 mL, 1.2 mmol) was dissolved in 5 mL of dry THF. The reaction mixture was cooled down to −78 °C and compound **44** (0.35 g, 1 mmol) (dissolved in 1 mL of dry THF) was added. The reaction mixture was warmed to −35 °C during 1 h and then cooled back to −78 °C. Ethyl iodide (0.10 mL, 1.3 mmol) was added and the reaction mixture was warmed to room temperature during 2 h and left stirring overnight. 37% HCl in water (0.27 mL, 3.2 mmol) was added and stirred for 3 h. The reaction mixture was extracted with DCM/H_2O, dried with $MgSO_4$, and evaporated. The product was purified by column chromatography with DCM as eluent. Yield = 0.24 g (89%). ^{1}H NMR (400 MHz, $CDCl_3$) δ: 7.67 (s,1H), 7.11 (s, 1H), 3.88 (s, 3H), 3.35–3.25 (m, 1H), 2.81 (ABX, $J = 19.2$ Hz^a, $J = 7.2$ Hz^b, 1H), 2.32 (ABX, $J = 19.2$ Hz^a, $J = 3.2$ Hz^b, 1H), 1.95–1.85 (m, 1H), 1.55–1.45 (m, 1H), 0.93 (t, $J = 7.2$ Hz, 3H) ppm.

4.1.12. (1S)-5-bromo-3-methyl-2,3-dihydro-1H-inden-1-ol (**47**)

In a 50 mL round bottom flask under N_2 atmosphere, (*R*)-(+)-2-methyl-CBS-oxazaborolidine catalyst (73.9 mg, 0.27 mmol, 1 M in toluene) in anhydrous toluene (5 mL) was added to *N*,*N*-diethylaniline borane (1.58 mL, 8.88 mmol) at room temperature (25 °C). To this solution **42** (0.50 g, 2.22 mmol) in toluene (20 mL) was added dropwise over 5 h, and the resulting mixture was stirred overnight at room temperature (25 °C). Reaction was monitored by reverse phase UPLC (t_R: 0.59). The reaction mixture was carefully quenched with methanol (5 mL) and 1 M HCl (1 mL) and extracted with ethyl acetate (4 × 50 mL). The combined organic layer was washed with brine, dried over Na_2SO_4, and concentrated *in vacuo*. The white residue was purified by flash chromatography (0–30 % ethyl acetate/hexanes) to afford the white crystalline solid **47** as a racemic mixture of diastereomers in a ratio 3:5. Yield = 0.49 g, 2.16 mmol (97%). ^{1}H NMR (400 MHz, $CDCl_3$) δ: 7.41–7.32 (m, 3H), 7.29–7.22 (m, 3H), 5.20 (dd, $J = 6.4$, 3.1 Hz, 1H), 5.16–5.08 (m, 1H), 3.43 (h, $J = 7.0$ Hz, 1H), 3.05 (h, $J = 7.1$ Hz, 1H), 2.76 (dt, $J = 12.7$, 7.1 Hz, 1H), 2.25 (ddd, $J = 13.6$, 7.4, 3.1 Hz, 1H), 1.98 (dt, $J = 13.4$, 6.6 Hz, 1H), 1.49 (ddd, $J = 12.7$, 8.9, 7.6 Hz, 1H), 1.34 (d, $J = 6.8$ Hz, 3H), 1.26 (dd, $J = 7.1$, 2.4 Hz, 2H) ppm. HPLC (Chiralpak AD-H column, 10% MeOH with 20 nM NH_3, 90% CO_2, 3.0 mL/min, 254 nm, ee = 95.8%. UPLC-MS: 209^+, 211^+; t_R: 1.91 min.

4.1.13. (1R)-5-bromo-3-methyl-2,3-dihydro-1H-inden-1-ol (**48**)

In a 50 mL round bottom flask under N_2, (*S*)-(+)-2-methyl-CBS-oxazaborolidine catalyst (73.9 mg, 0.27 mmol, 1 M in toluene) in anhydrous toluene (5 mL) was added to *N*,*N*-diethylaniline borane (1.58 mL, 8.88 mmol) at room temperature (25 °C). To this solution **42** (0.50 g, 2.22 mmol) in toluene (20 mL) was added dropwise over 5 h, and the resulting mixture was stirred overnight at room temperature (25 °C). The reaction was monitored by reverse phase UPLC (t_R: 0.58). The reaction mixture was carefully quenched with methanol (5 mL) and 1 N HCl (1 mL) and then extracted with ethyl acetate (4 × 50 mL). The combined organic layer washed with brine, dried over Na_2SO_4, and concentrated *in vacuo*. The white residue was purified by flash chromatography (0–30 % ethyl acetate/hexanes) to afford the white crystalline solid **48** as a racemic mixture in a ratio (3:5). Yield = 0.50 g, 2.20 mmol (99%). ^{1}H NMR (400 MHz, $CDCl_3$) δ: 7.37 (dddt, $J = 8.4$, 5.6, 2.8, 1.2 Hz, 4H), 7.28–7.22 (m, 2H), 5.20 (dd, $J = 6.4$, 3.1 Hz, 1H), 5.12 (t, $J = 7.3$ Hz, 1H), 3.43 (h, $J = 7.0$ Hz, 1H), 3.12–2.97 (m, 1H), 2.76 (dt, $J = 12.7$, 7.1 Hz, 1H), 2.25 (ddd, $J = 13.6$, 7.4, 3.1 Hz, 1H), 1.98 (dt, $J = 13.4$, 6.6 Hz, 1H), 1.49 (ddd, $J = 12.7$, 8.9, 7.7 Hz, 1H), 1.34 (d, $J = 6.8$ Hz, 3H), 1.26 (d, $J = 7.0$ Hz, 2H) ppm. HPLC (Chiralpak AD-H column, 10% MeOH with 20 nM NH_3, 90% CO_2, 3.0 mL/min, 254 nm, ee = 96.2%. UPLC-MS: 209^+, 211^+; t_R: 1.92, 1.95 min.

4.1.14. N-((1R,3S)-3-isopropyl-3-(7-(trifluoromethyl)-1,2,3,4-tetrahydroisoquinoline-2-carbonyl)cyclopentyl)-2-nitrobenzenesulfonamide (**49**)

In a 50 mL round bottom flask, to a solution of amine **6** (1.00 g, 2.82 mmol) in anhydrous CH_2Cl_2 (10 mL) was added 2-nitrobenzenesulfonyl chloride (0.75 mg, 3.38 mmol) followed by DIPEA (1.70 mL, 9.73 mmol) and stirred at room temperature (25 °C) for 1 h. The reaction was monitored by reverse phase UPLC (t_R: 0.77). The reaction mixture was concentrated *in vacuo* to obtained the crude product (yellow oil). The product was purified by flash chromatography (40–80 % ethyl acetate/hexanes) to afford the light yellow foamy solid **49**. Yield = 1.50 g (98%).^{1}H NMR (400 MHz, $CDCl_3$) δ: 8.16–8.09 (m, 1H), 7.82–7.75 (m, 1H), 7.75–7.64 (m, 2H), 7.48–7.40 (m, 1H), 7.36 (s, 1H), 7.27 (d, $J = 4.9$ Hz, 1H), 6.05 (s, 1H), 4.81 (s, 1H), 4.71 (d, $J = 16.4$ Hz, 1H), 3.94 (d, $J = 16.7$ Hz, 1H), 3.81 (dq, $J = 8.7$, 4.3 Hz, 1H), 3.76–3.64 (m, 1H), 2.90 (tt, $J = 16.6$, 6.4 Hz, 2H), 2.40 (d, $J = 12.9$ Hz, 1H), 2.14 (pent., $J = 6.7$ Hz, 1H), 1.82 (d, $J = 16.1$ Hz, 3H), 1.67 (dd, $J = 8.6$, 4.5 Hz, 1H), 1.58–1.40 (m, 1H), 0.87 (d, $J = 6.7$ Hz, 3H), 0.76 (d, $J = 6.7$ Hz, 3H) ppm. UPLC-MS: 540^+; t_R: 2.85 min.

4.1.15. N-((1R)-5-bromo-3-methyl-2,3-dihydro-1H-inden-1-yl)-N-((1R,3S)-3-isopropyl-3-(7-(trifluoromethyl)-1,2,3,4-tetrahydroisoquinoline-2-carbonyl)cyclopentyl)-2-nitrobenzenesulfonamide (**50**)

In a 100 mL round-bottom flask, to a cooled solution (−78 °C, acetone/dry ice bath) of PPh_3 (1.23 g, 4.69 mmol) in anhydrous THF (20 mL) was added DEAD (0.82 g, 4.69 mmol) and stirred for 30 min, followed by addition of **47** (0.40 g, 1.76 mmol). The pink colored reaction mixture was allowed to stir for 30 min maintaining the temperature at −78 °C. To this solution, **49** (0.63 g, 1.17 mmol) was added. The reaction mixture was stirred for 6 h at −78 °C and allowed to warm up to room temperature overnight. The reaction was monitored by reverse phase UPLC (t_R: 0.93). The reaction mixture was concentrated *in vacuo* to obtained a pink-colored residue. The crude residue was purified by flash chromatography (0–10 % CH_2Cl_2/MeOH) to afford the light pink foamy solid **50** (purity 80%). Yield = 1.00 g (<100%). UPLC-MS: 540^+; t_R: 3.53 min. Without further purification, **50** was taken forward in the following deprotection step.

4.1.16. N-((1S)-5-bromo-3-methyl-2,3-dihydro-1H-inden-1-yl)-N-((1R,3S)-3-isopropyl-3-(7-(trifluoromethyl)-1,2,3,4-tetrahydroisoquinoline-2-carbonyl)cyclopentyl)-2-nitrobenzenesulfonamide (**51**)

In a 100 mL round-bottom flask, to a cooled solution (−78 °C, acetone/dry ice bath) of PPh_3 (1.23 g, 4.69 mmol) in anhydrous THF (20 mL) was added DEAD (0.82 g, 4.69 mmol) and stirred for 30 min, followed by addition of **48** (0.40 g, 1.76 mmol). The pink colored reaction mixture was allowed to stir for 30 min maintaining the temperature at −78 °C. To this solution, **49** (0.63 g, 1.17 mmol) was added. The reaction mixture was stirred for 6 h at −78 °C and allowed to warm up to room temperature overnight. The reaction was monitored by reverse phase UPLC (t_R: 0.93). The reaction mixture was concentrated *in vacuo* to obtained a pink color residue. The crude residue was purified by flash chromatography (0–10 % CH_2Cl_2/MeOH) to afford the light pink foamy solid **55** (purity 80%). Yield = 1.00 g (<100%). UPLC-MS: 540^+; t_R: 3.53 min. Without further purification, **51** was taken forward in the following deprotection step.

*4.1.17. (1S,3R)-N-(3,5-bis(trifluoromethyl)benzyl)-3-(((1S,3R)-5-bromo-3-methyl-2,3-dihydro-1H-inden-1-yl)amino)-1-isopropylcyclopentanecarboxamide (**37a**) and (1S,3R)-N-(3,5-bis(trifluoromethyl)benzyl)-3-(((1S,3S)-5-bromo-3-methyl-2,3-dihydro-1H-inden-1-yl)amino)-1-isopropylcyclopentanecarboxamide (**37b**)*

In a 20 mL scintillation vial, to a solution of **50** (1.00 g, 1.34 mmol) in DMF (10 mL) was added K_2CO_3 (0.55 g, 4.01 mmol) and benzenethiol (274.4 μL, 2.67 mmol), and the reaction mixture was stirred at room temperature for 30 min. The reaction was monitored by reverse phase UPLC (t_R: 0.73 and 0.74). To the reaction mixture was added water (20 mL) followed by extraction with CH_2Cl_2 (4 × 100 mL). The combined organic layer was washed with water, brine, dried over Na_2SO_4, and concentrated *in vacuo*. The brown residue was purified by flash chromatography (0–10% CH_2Cl_2/MeOH) to afford **37a** (0.10 g) and **37b** (0.10 g) with 80% diastereomeric excess purity by SFC analysis. Further purification was carried out by reverse–phase preparatory HPLC-UV with a gradient from 1 to 99% mobile phase B (mobile phase A = 0.1% HCl in water, mobile phase B = 0.1% HCl in CH_3CN) resulting in pure **37a** HCl salt and **37b** HCl salt as a white solid. Yield: **37a** = 14.7 mg, 1.8%, UPLC-MS: 563^+, 565^+; t_R: 2.45 min and **37b** = 17.3 mg, 2.1%, UPLC-MS: 563^+, 565^+; t_R: 2.49 min.

*4.1.18. (1S,3R)-N-(3,5-bis(trifluoromethyl)benzyl)-3-(((1R,3R)-5-bromo-3-methyl-2,3-dihydro-1H-inden-1-yl)amino)-1-isopropylcyclopentanecarboxamide (**37c**) and (1S,3R)-N-(3,5-bis(trifluoromethyl)benzyl)-3-(((1R,3S)-5-bromo-3-methyl-2,3-dihydro-1H-inden-1-yl)amino)-1-isopropylcyclopentanecarboxamide (**37d**)*

In a 20 mL scintillation vial, to a solution of **51** (1.00 g, 1.34 mmol) in DMF (10 mL) was added K_2CO_3 (0.55 g, 4.01 mmol) and benzenethiol (274.4 μL, 2.67 mmol), and the reaction mixture was stirred at room temperature for 30 min. The reaction was monitored by reverse phase UPLC (t_R: 0.76). To the reaction mixture was added water (20 mL) followed by extraction with CH_2Cl_2 (4 × 100 mL). The combined organic layer was washed with water, brine, dried over Na_2SO_4, and concentrated *in vacuo*. The brown residue was purified by flash chromatography (0–10% CH_2Cl_2/MeOH) to afford **37c** (50 mg) and **37d** (90 mg) both with 50% diastereomeric excess purity. Further purification was carried out by reverse–phase preparatory HPLC-UV with a gradient from 1 to 99% mobile phase B (mobile phase A = 0.1% HCl in water, mobile phase B = 0.1% HCl in CH_3CN) resulting in **37c** HCl salt and **37d** HCl salt as a white solid, both again with 70% diastereomeric excess purity. Therefore further purification was carried out on a Gilson purification instrument with a normal phase silica column and a diode array detector using a Luna Phenomenex column (50 mm × 21 mm, 5 μm), and a linear gradient from 1 to 10% (CH_2Cl_2/MeOH) of mobile phase was applied. Mobile phase A consisted of CH_2Cl_2 and mobile phase B consisted of 10% MeOH/CH_2Cl_2. Yield: **37c** = 13.1 mg, 1.7%, UPLC-MS: 563^+, 565^+; t_R: 2.52 min **37d** = 12.7 mg, 1.7%, UPLC-MS: 563^+, 565^+; t_R: 2.52 min.

4.2. Pharmacology

4.2.1. Chemicals and reagents

^{125}I-CCL2 (2200 Ci/mmol) was purchased from Perkin–Elmer (Waltham, MA). INCB3344 was synthesized as described previously [27,28]. [^{3}H]INCB3344 (specific activity 32 Ci/mmol) was custom-labeled by Vitrax (Placentia, CA) for which a dehydrogenated precursor of INCB3344 was provided. Tango™ CCR2-*bla* U2OS cells stably expressing human CCR2 were obtained from Invitrogen (Carlsbad, CA).

4.2.2. Cell culture and membrane preparation

U2OS cells stably expressing the human CCR2 receptor (Invitrogen, Carlsbad, CA) were cultured in McCoys5a medium supplemented with 10% fetal calf serum, 2 mM glutamine, 0.1 mM non-essential amino acids (NEAA), 25 mM HEPES, 1 mM sodium pyruvate, 100 IU/mL penicillin, 100 μg/mL streptomycin, 100 μg/mL G418, 50 μg/mL hygromycin and 125 μg/mL zeocin in a humidified atmosphere at 37 °C and 5% CO_2. Cell culture and membrane preparation were performed as described previously [18].

4.2.3. ^{125}I-CCL2 displacement assay

Binding assays were performed as described previously [18]. Briefly, 15 μg of U2OS–CCR2 membranes were incubated for 150 min with 0.1 nM ^{125}I-CCL2 in the absence or presence of competing ligand at 37 °C.

4.2.4. [^{3}H]INCB3344 dual point competition association assay

Kinetic rate index (KRI) values of unlabeled ligands were determined using the dual-point competition association assay as described previously [12]. Briefly, 10 μg of U2OS–CCR2 membranes were incubated for 50 min (t_1) or 240 min (t_2) with 1.8 nM [^{3}H]-INCB3344 in the absence or presence of unlabeled ligands at 25 °C. The amount of radioligand bound to the receptor was measured after co-incubation of the unlabeled ligands at 1-fold their respective K_i value in the ^{125}I-CCL2 displacement assay. KRI values of unlabeled ligands were calculated using eq. (1), as mentioned below in the Data Analysis section.

4.2.5. [^{3}H]INCB3344 competition association assay

The kinetic parameters of unlabeled ligands were determined using the competition association assay described earlier by our group [12]. Briefly, at different time points, 10 μg of U2OS–CCR2 membranes was added to 1.8 nM [^{3}H]-INCB3344 in a total volume of 100 μL of assay buffer in the absence or presence of competing ligand at 25 °C. Kinetic parameters of unlabeled ligands were calculated using eq. (2), as mentioned below in the Data Analysis section.

4.2.6. [^{35}S]GTPγS binding assay

Ten micrograms of membranes were diluted in 100 μL of assay buffer containing 50 mM Tris-HCl buffer (pH 7.4), 5 mM $MgCl_2$, 100 mM NaCl, 1 mM EDTA, 0.05% bovine serum albumin, 10 μM GDP, and 10 μg of saponin per assay point. The membranes were preincubated with 10 μM of antagonist for 30 min at 25 °C. Then CCL2 (10 nM) was added, followed by another incubation of 30 min; finally, the mixture was incubated for 90 min after the addition of [^{35}S]GTPγS (0.3 nM). The incubation was terminated by dilution with ice-cold 50 mM Tris-HCl buffer supplemented with 5 mM $MgCl_2$. Separation of bound from free radioligand was performed by rapid filtration through Whatman GF/B filters using a Brandel harvester. Filters were subsequently washed three times with ice-cold buffer. Filter-bound radioactivity was measured by scintillation spectrometry (LKB Wallac, 1219 Rackbeta) after addition of 3.5 mL of Packard Emulsifier Safe.

4.2.7. Data analysis

All experiments were analyzed using the nonlinear regression curve fitting program Prism 5 (GraphPad, San Diego, CA). For radioligand displacement data K_i values were calculated from IC_{50} values using the Cheng and Prusoff equation [29]. KRI values were calculated by dividing the specific radioligand binding measured at t_1 (B_{t1}) by its binding at t_2 (B_{t2}) in the presence of unlabeled competing ligand as follows:

$$KRI = B_{t1}/B_{t2} \quad (1)$$

Data presented are the mean ± S.E.M. of at least 3 experiments performed in duplicate. Statistical analysis was performed with a two-tailed unpaired Student's *t*-test.

Association and dissociation rates for unlabeled ligands were determined by nonlinear regression analysis of the competition association data as described by Motulsky and Mahan,

$$K_A = k_1[L]\cdot 10^{-9} + k_2$$
$$K_B = k_3[I]\cdot 10^{-9} + k_4$$
$$S = \sqrt{(K_A - K_B)^2 + 4\cdot k_1\cdot k_3\cdot L\cdot I\cdot 10^{-18}}$$
$$K_F = 0.5(K_A + K_B + S)$$
$$K_S = 0.5(K_A + K_B - S)$$
$$Q = \frac{B_{\max}\cdot k_1\cdot L\cdot 10^{-9}}{K_F - K_S}$$
$$Y = Q\cdot\left(\frac{k_4\cdot(K_F - K_S)}{K_F\cdot K_S} + \frac{k_4 - K_F}{K_F}e^{(-K_F\cdot X)} - \frac{k_4 - K_S}{K_S}e^{(-K_S\cdot X)}\right) \quad (2)$$

where X is the time (min), Y is the specific binding (disintegrations per minute (DPM)), k_1 is k_{on} (M^{-1} min^{-1}) of [^{3}H]-INCB3344 predetermined in association experiments, k_2 is k_{off} (min^{-1}) of [^{3}H]-INCB3344 predetermined in dissociation experiments, L is the concentration of [^{3}H]-INCB3344 used (nM), B_{max} is the total binding (DPM), and I is the concentration of unlabeled ligand (nM). Fixing these parameters into eq. (2) allows for the following parameters to be calculated: k_3 is k_{on} (M^{-1} min^{-1}) of the unlabeled ligand, and k_4 is k_{off} (min^{-1}) of the unlabeled ligand. The association and dissociation rates were used to calculate the "kinetic K_D" as follows:

$$K_D = k_{off}/k_{on} \quad (3)$$

The RT was calculated according to the formula RT = $1/k_{off}$.

Acknowledgment

This study was financially supported by the Dutch Top Institute Pharma, project number D1-301. We thank Dr. Julien Louvel and Jacobus van Veldhoven for their input in analytical data analysis and helpful comments. We acknowledge Dong Guo and Prof. Dr. Martine Smit (Vrije Universiteit, Amsterdam, The Netherlands) for helpful comments and suggestions.

Appendix A. Supplementary data

Supplementary data related to this article can be found at http://dx.doi.org/10.1016/j.ejmech.2015.01.063.

References

[1] D. D'Ambrosio, P. Panina-Bordignon, F. Sinigaglia, Chemokine receptors in inflammation: an overview, J. Immunol. Methods 273 (2003) 3–13.
[2] Y.S. Kang, J.J. Cha, Y.Y. Hyun, D.R. Cha, Novel C-C chemokine receptor 2 antagonists in metabolic disease: a review of recent developments, Expert Opin. Inv Drug 20 (2011) 745–756.
[3] I.F. Charo, R.M. Ransohoff, The many roles of chemokines and chemokine receptors in inflammation, N. Engl. J. Med. 354 (2006) 610–621.
[4] M. Feria, F. Diaz-Gonzalez, The CCR2 receptor as a therapeutic target, Expert Opin. Ther. Pat. 16 (2006) 49–57.
[5] M. Struthers, A. Pasternak, CCR2 antagonists, Curr. Top. Med. Chem. 10 (2010) 1278–1298.
[6] J. Kalliomaki, N. Attal, B. Jonzon, F.W. Bach, K. Huizar, S. Ratcliffe, B. Eriksson, M. Janecki, A. Danilov, D. Bouhassira, A randomized, double-blind, placebo-controlled trial of a chemokine receptor 2 (CCR2) antagonist in posttraumatic neuralgia, Pain 154 (2013) 761–767.
[7] A. Kalinowska, J. Losy, Investigational C-C chemokine receptor 2 antagonists for the treatment of autoimmune diseases, Expert Opin. Inv Drug 17 (2008) 1267–1279.
[8] C.E. Vergunst, D.M. Gerlag, L. Lopatinskaya, L. Klareskog, M.D. Smith, F. van den Bosch, H.J. Dinant, Y. Lee, T. Wyant, E.W. Jacobson, D. Baeten, P.P. Tak, Modulation of CCR2 in rheumatoid arthritis: a double-blind, randomized, placebo-controlled clinical trial, Arthritis Rheum. 58 (2008) 1931–1939.
[9] J. Gilbert, J. Lekstrom-Himes, D. Donaldson, Y. Lee, M.X. Hu, J. Xu, T. Wyant, M. Davidson, M.S. Grp, Effect of CC chemokine receptor 2 CCR2 blockade on serum C-reactive protein in individuals at atherosclerotic risk and with a single nucleotide polymorphism of the monocyte chemoattractant Protein-1 promoter region, Am. J. Cardiol. 107 (2011) 906–911.
[10] R.A. Copeland, D.L. Pompliano, T.D. Meek, Drug-target residence time and its implications for lead optimization, Nat. Rev. Drug Discov. 5 (2006) 730–739.
[11] D.C. Swinney, Biochemical mechanisms of drug action: what does it take for success? Nat. Rev. Drug Discov. 3 (2004) 801–808.
[12] M. Vilums, A.J. Zweemer, Z. Yu, H. de Vries, J.M. Hillger, H. Wapenaar, I.A. Bollen, F. Barmare, R. Gross, J. Clemens, P. Krenitsky, J. Brussee, D. Stamos, J. Saunders, L.H. Heitman, A.P. Ijzerman, Structure-kinetic relationships—an overlooked parameter in hit-to-lead optimization: a case of cyclopentylamines as chemokine receptor 2 antagonists, J. Med. Chem. 56 (2013) 7706–7714.
[13] E. Frerot, J. Coste, A. Pantaloni, M.N. Dufour, P. Jouin, Pybop and Pybrop - 2 reagents for the difficult coupling of the Alpha,Alpha-dialkyl amino-acid, Aib, Tetrahedron 47 (1991) 259–270.
[14] E.R. Burkhardt, B.M. Coleridge, Reductive amination with 5-ethyl-2-methylpyridine borane, Tetrahedron Lett. 49 (2008) 5152–5155.
[15] P. Zhang, J.C. Kern, E.A. Terefenko, E.J. Trybulski, 5-Aryl-indan-1-ol and analogs useful as progesterone receptor modulators., in: Patent US2007066628.
[16] S.H. Lee, I.S. Kim, Q.R. Li, G.R. Dong, L.S. Jeong, Y.H. Jung, Stereoselective amination of chiral benzylic ethers using chlorosulfonyl isocyanate: total synthesis of (+)-Sertraline, J. Org. Chem. 76 (2011) 10011–10019.
[17] T. Fukuyama, M. Cheung, C.K. Jow, Y. Hidai, T. Kan, 2,4-dinitrobenzenesulfonamides: a simple and practical method for the preparation of a variety of secondary amines and diamines. Tetrahedron Lett. 38 (1997) 5831–5834.
[18] A.J.M. Zweemer, I. Nederpelt, H. Vrieling, S. Hafith, M.L.J. Doornbos, H. de Vries, J. Abt, R. Gross, D. Stamos, J. Saunders, M.J. Smit, A.P. IJzerman, L.H. Heitman, Multiple binding sites for small-molecule antagonists at the CC chemokine receptor 2, Mol. Pharmacol. 84 (2013) 551–561.
[19] S. Kothandaraman, K.L. Donnely, G. Butora, R. Jiao, A. Pasternak, G.J. Morriello, S.D. Goble, C. Zhou, S.G. Mills, M. Maccoss, P.P. Vicario, J.M. Ayala, J.A. Demartino, M. Struthers, M.A. Cascieri, L. Yang, Design, synthesis, and structure-activity relationship of novel CCR2 antagonists, Bioorg. Med. Chem. Lett. 19 (2009) 1830–1834.
[20] C. Zheng, G. Cao, M. Xia, H. Feng, J. Glenn, R. Anand, K. Zhang, T. Huang, A. Wang, L. Kong, M. Li, L. Galya, R.O. Hughes, R. Devraj, P.A. Morton, D.J. Rogier, M. Covington, F. Baribaud, N. Shin, P. Scherle, S. Diamond, S. Yeleswaram, K. Vaddi, R. Newton, G. Hollis, S. Friedman, B. Metcalf, C.B. Xue, Discovery of INCB10820/PF-4178903, a potent, selective, and orally bioavailable dual CCR2 and CCR5 antagonist, Bioorg. Med. Chem. Lett. 21 (2011) 1442–1446.
[21] R. Jiao, S.D. Goble, S.G. Mills, G. Morriello, A. Pasternak, L. Yang, C. Zhou, G. Butora, S. Kothandaraman, D. Guiadeen, C. Moyes, Tetrahydropyranyl cyclopentyl tetrahydropyridopyridine modulators of chemokine receptor activity., in: Patent WO03093231.
[22] D. Guo, E.J.H. van Dorp, T. Mulder-Krieger, J.P.D. van Veldhoven, J. Brussee, A.P. IJzerman, L.H. Heitman, Dual-Point competition association assay: a fast and high-throughput kinetic screening method for assessing ligand-receptor binding kinetics, J. Biomol. Screen. 18 (2013) 309–320.
[23] C.B. Xue, A.L. Wang, Q. Han, Y.X. Zhang, G.F. Cao, H. Feng, T.S. Huang, C.S. Zheng, M. Xia, K. Zhang, L.Q. Kong, J. Glenn, R. Anand, D. Meloni, D.J. Robinson, L.X. Shao, L. Storace, M. Li, R.O. Hughes, R. Devraj, P.A. Morton, D.J. Rogier, M. Covington, P. Scherle, S. Diamond, T. Emm, S. Yeleswaram, N. Contel, K. Vaddi, R. Newton, G. Hollis, B. Metcalf, Discovery of INCB8761/PF-4136309, a potent, selective, and orally bioavailable CCR2 antagonist, ACS Med. Chem. Lett. 2 (2011) 913–918.
[24] A. Pasternak, S.D. Goble, M. Struthers, P.P. Vicario, J.M. Ayala, J. Di Salvo, R. Kilburn, T. Wisniewski, J.A. Demartino, G.S. Mills, L. Yang, Discovery of a potent orally bioavailable CCR2 and CCR5 dual antagonist, ACS Med. Chem. Lett. 1 (2010) 14–18.
[25] P. Schmidtke, F.J. Luque, J.B. Murray, X. Barril, Shielded hydrogen bonds as structural determinants of binding kinetics: application in drug design, J. Am. Chem. Soc. 133 (2011) 18903–18910.
[26] G. Butora, S.D. Goble, A. Pasternak, L. Yang, C. Zhou, C.R. Moyes, Heterocyclic Cyclopentyl Tetrahydroisoquinoline And Tetrahydropyridopyridine Modulators Of Chemokine Receptor Activity., in: Patent WO 2004094371, 2004.
[27] C.M. Xue, B.; Feng, H.; Cao, G.; Huang, T.; Zheng, C.; Robinson, D. J.; Han, A., 3-Aminopyrrolidine derivatives as modulators of chemokine receptors., in: Patent WO2004050024.
[28] C.M. Brodmerkel, R. Huber, M. Covington, S. Diamond, L. Hall, R. Collins, L. Leffet, K. Gallagher, P. Feldman, P. Collier, M. Stow, X. Gu, F. Baribaud, N. Shin, B. Thomas, T. Burn, G. Hollis, S. Yeleswaram, K. Solomon, S. Friedman, A. Wang, C.B. Xue, R.C. Newton, P. Scherle, K. Vaddi, Discovery and pharmacological characterization of a novel rodent-active CCR2 antagonist, INCB3344, J. Immunol. 175 (2005) 5370–5378.
[29] Y. Cheng, W.H. Prusoff, Relationship between inhibition constant (K1) and concentration of inhibitor which causes 50 per cent inhibition (I50) of an enzymatic-reaction, Biochem. Pharmacol. 22 (1973) 3099–3108.